JOURNAL OF COMPUTATIONAL PHYSICS **138,** 224–247 (1997)
ARTICLE NO. CP975842

The Dynamics of an Elastic Membrane Using the Impulse Method

R. Cortez*,[1] and D. A. Varela†

*Courant Institute of Mathematical Sciences, New York University, 251 Mercer Street, New York, New York 10012; and
†Department of Engineering and Applied Science, California Institute of Technology, Pasadena, California 91125
E-mail: cortezr@cims.nyu.edu

Received March 20, 1997; revised August 28, 1997

A validation study of the impulse method applied to the motion of a closed elastic membrane under tension separating two incompressible, inviscid fluids in two dimensions is presented. The approach consists of a nonlinear analysis based on a small-amplitude perturbation of an exact solution. The equations of motion for the Fourier coefficients of the solution are developed to two orders beyond the leading-order problem. The nonlinear terms in the equations depict the coupling of the Fourier modes and account for the temporal variation of the tension. The last order of the expansion is used to compute frequency corrections to the driving modes. Solutions for various problems are found and compared with a numerical method based on impulse variables. The results show that the numerical periods and amplitudes of the oscillations approach the values predicted by the perturbation analysis as the numerical smoothing parameter is reduced. This validates the use of impulse methods for free-boundary motion with surface forces.

Key Words: impulse method; particle methods; perturbation analysis.

1. INTRODUCTION

Many physical phenomena involve interfaces between two fluids moving under the influence of forces acting at the immersed boundaries. In this paper we address

[1] This author was partly supported in Berkeley by the Applied Mathematical Sciences subprogram of the Office of Energy Research, U.S. Department of Energy, under Contract DE-AC03-76SF00098 and by the Air Force Office of Scientific Research AASERT Grant FDF49620-93-1-0053; in New York by the National Science Foundation through a Mathematical Sciences Postdoctoral Fellowship and by the U.S. Department of Energy Grant DE-FG02-96ER25287.

0021-9991/97 $25.00

the problem of the interaction of a closed, flexible, elastic membrane with incompressible fluids inside and outside. The forces along the membrane are proportional to its curvature multiplied by a tension, which depends on the length of the membrane and is therefore time-dependent. The goal of this paper is twofold: (a) to develop approximate equations whose solution describes the motion of a closed elastic membrane separating two fluids of different densities; and (b) to use the results to test the validity of a numerical method based on impulse variables.

In the first part of the paper we present a nonlinear analysis of the problem based on a small-amplitude perturbation using a circular membrane as the base solution. A similar technique was used in [21] for the study of bubble oscillations in three dimensions. The forces in their case include only the case of constant tension. In our analysis, the region inside the membrane is initially mapped to the unit disc to simplify the enforcement of boundary conditions. The analytical techniques used to obtain the small-amplitude dynamics of the interface are the classical methods of singular perturbation analysis [15, 20]. As in the typical problems involving periodic forcing, we apply the method of multiple scales or the Lindstedt–Poincaré method for removing secular behavior from the perturbation equations, thus rendering a solution valid uniformly in time. The expansions are carried out to the third order in ε (the perturbation amplitude) so that corrections to the leading-order frequencies can be calculated from the multiple scale analysis. This provides the nonlinear relation between the oscillation period and the amplitude of the motion. The solutions to the perturbation equations provide approximate solutions to the original problem independent of any numerical method and, therefore, can be used to test the validity of specific methods. The solutions for two different cases of the tension are presented in Section 3.

Numerical methods developed to model this type of problem include the Lagrangian method based on impulse variables described in [9]. In this method, particles carrying impulse density are distributed along the membrane. For inviscid flows, the impulse defined at the interface is sufficient to describe the entire motion and thus the discretization of the impulse is only necessary on a one-dimensional set. Impulse is a very natural variable to transmit the effect of the boundary forces to the fluid. An important feature of the impulse method is that it can be used to model viscous flows in a straightforward manner and may have an advantage over other particle methods (especially in three dimensions) due to the divergence-free character of the induced vorticity field (see [7] for details). To our knowledge the present paper is the first analysis of the impulse method solutions in the context of immersed boundaries. The impulse method is described in Section 4 and the numerical results are presented in Section 5.

The corrected oscillation frequencies resulting from the perturbation analysis provide a good basis for comparison with the results of the numerical method for moderate perturbation amplitudes. Figure 1 shows an example comparing the dynamics of a membrane over two periods of oscillation. The solid curve is the result of the asymptotic analysis and the dashed curve was obtained using the impulse method. The initial condition was a circle plus a third-mode perturbation of amplitude 0.1. This comparison illustrates clearly the effects of smoothing parameters of the numerical method on the period of the motion. Our results show that

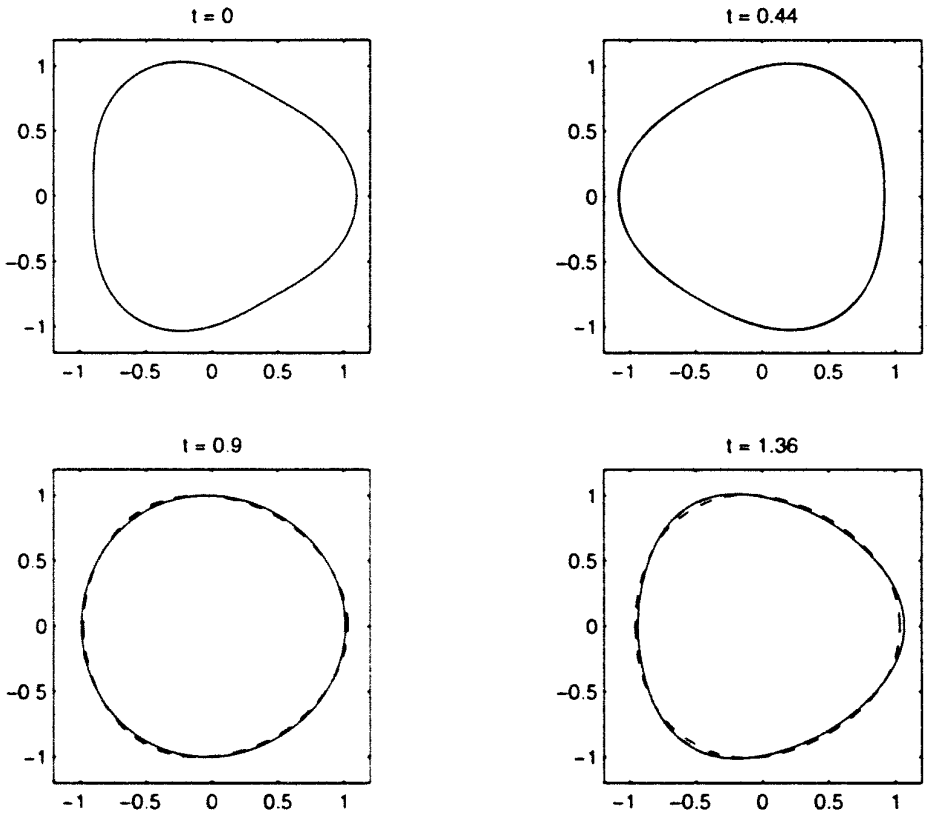

FIG. 1. Comparison of membrane motion given by the impulse method (dashed) and the asymptotic solution (solid) over two periods. Initial conditions are given by $r(\theta) = r_o + 0.1\cos(3\theta)$. The figure shows a lag in the numerical solution due to the smoothing parameter.

the impulse method yields solutions which are in good agreement with solutions of the perturbation equations. The numerical periods are slightly longer than the analytical ones, due to the smoothing parameter in the method. As this parameter is reduced, the computed periods and amplitudes of the oscillations approach the asymptotic ones.

Different versions of the problem presented in this paper are used as models for various physical phenomena. Models of the flow of blood in the heart chambers have been developed by Peskin and his collaborators (see, e.g., [14, 17, 18]) in two and three dimensions. The models treat the walls of the heart as elastic membranes interacting with a fluid. Similar models have also been adapted to study the locomotion of aquatic animals and microorganisms [10, 11]. The motion of bubbles has been studied asymptotically in [21] and numerically in [6] for the case of constant tension.

2. THE EQUATIONS OF MOTION

The general problem we consider consists of two incompressible, inviscid fluids in the plane separated by a closed membrane under tension (see Fig. 2). The fluids

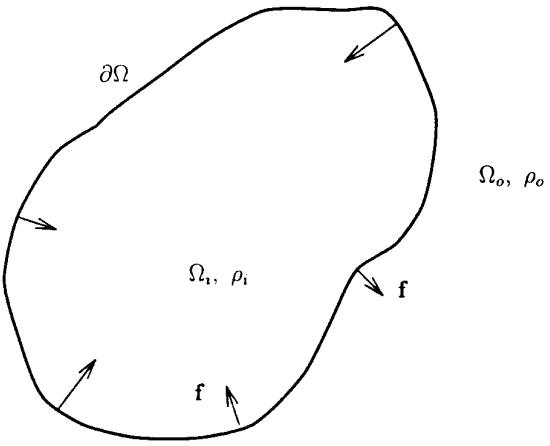

FIG. 2. Diagram of an elastic membrane separating two fluids.

inside and outside the membrane have constant but possibly different densities ρ_i and ρ_o. The fluid interface is the membrane, which is assumed to be massless, infinitely thin and moving with the fluid velocity. The tension is assumed to be a function of the membrane length and, therefore, time-dependent.

Let Ω_i and Ω_o represent respectively the regions inside and outside the membrane. Since the flow is irrotational in both Ω_i and Ω_o, the flow in these regions is described by two velocity potentials which satisfy

$$\Delta\phi = 0 \quad \text{in } \Omega_i$$
$$\Delta\psi = 0 \quad \text{in } \Omega_o.$$

Define a function (in polar coordinates) $f(r, \theta) = r - R(\theta, t)$, whose zero level set is the interface $\partial\Omega$. The function $R(\theta, t)$ is assumed to be single-valued in θ. There are three conditions that must be satisfied on the interface $\partial\Omega$:

1. The membrane must define the interface between the two fluids at all times and should always consist of the same material particles. Thus we require continuity of the normal velocity,

$$\frac{\partial\phi}{\partial n} = \frac{\partial\psi}{\partial n} \Rightarrow \hat{n} \cdot (\nabla\phi - \nabla\psi) = 0,$$

where the unit normal vector $\hat{n}$ is the normalized gradient of f.

2. The membrane must move with the fluid velocity

$$\frac{\partial f}{\partial t} + \mathrm{u} \cdot \nabla f = 0.$$

3. The pressure jump at the interface must balance the elastic forces. The force density is assumed to be of the form

$$\sigma(L(t) - 2\pi R_0)\kappa,$$

where σ is a positive stiffness constant, $L(t)$ is the length of the membrane, $2\pi R_0$ is the length of the unstretched membrane, and κ is the curvature. The stiffness σ can be treated as a time-dependent function without any complications; however, here we restrict our attention to constant stiffness.

For simplicity and without loss of generality we assume that the area enclosed by the membrane equals π so that an exact solution of the problem is a circular membrane of unit radius. We also introduce the transformation $x = r/R$ which maps the inner region Ω_i to the unit disc. After the transformation the potential $\phi(x, \theta, t)$ must satisfy the equation for $0 \le x < 1$,

$$\left[1 + \left(\frac{R_\theta}{R}\right)^2\right]\phi_{xx} + \frac{1}{x}\left[1 - \left(\frac{R_\theta}{R}\right)_\theta + \left(\frac{R_\theta}{R}\right)^2\right]\phi_x + \frac{1}{x^2}\phi_{\theta\theta} - \frac{2}{x}\left(\frac{R_\theta}{R}\right)\phi_{x\theta} = 0, \quad (1)$$

where subscripts represent derivatives. $\psi(x, \theta, t)$ satisfies the same equation as ϕ but for $x > 1$. The three conditions at the interface $x = 1$ become:

1. The kinematic condition is

$$[R^2 + (R_\theta)^2](\phi - \psi)_x = RR_\theta(\phi - \psi)_\theta \quad (2)$$

2. The velocity of the fluid at the interface can be taken as the average of the velocities found from either side of the membrane; thus, $u = (\nabla\phi + \nabla\psi)/2$ and the second condition becomes

$$2R^3R_t + RR_\theta(\phi + \psi)_\theta = [R^2 + (R_\theta)^2](\phi + \psi)_x. \quad (3)$$

3. From Bernoulli's equation in each fluid, we find that the pressure inside and outside satisfies

$$p_0(x, t) = -\rho_i[\phi_t + \tfrac{1}{2}|\nabla\phi|^2] + P_0(t)$$
$$p_1(x, t) = -\rho_o[\psi_t + \tfrac{1}{2}|\nabla\psi|^2] + P_1(t).$$

We take the limit as x approaches 1 from both sides of the membrane and equate the pressure jump with the forces,

$$\rho_o[\psi_t + \tfrac{1}{2}|\nabla\psi|^2] - \rho_i[\phi_t + \tfrac{1}{2}|\nabla\phi|^2] + P_s(t) = \sigma(L(t) - 2\pi R_0)\kappa.$$

The quantity $P_s(t) = P_0(t) - P_1(t)$ accounts for all terms on the right-hand side of the last equation which depend solely on time. With this convention, when the right-hand side does not depend on position, the velocity potentials are identically zero.

We can nondimensionalize the problem and simplify the notation by making the following changes of variables:

$$\rho = \rho_o/\rho_i, \quad t' = t(\sigma/\rho_i)^{1/2}, \quad \phi' = \phi(\rho_i/\sigma)^{1/2}, \quad \psi' = \psi(\rho_i/\sigma)^{1/2}, \quad P_s'(t) = P_s(t)/\sigma.$$

The dynamic condition in terms of x is (after dropping the primes),

$$\frac{1}{R^4}\left[R^4(\rho\psi - \phi)_t - R^3R_t(\rho\psi - \phi)_x + \frac{1}{2}R^2(\rho(\psi_\theta)^2 - (\phi_\theta)^2) - RR_\theta(\rho\psi_\theta\psi_x - \phi_\theta\phi_x)\right.$$
$$\left. + \frac{1}{2}[R^2 + (R_\theta)^2][\rho(\psi_x)^2 - (\phi_x)^2]\right] = \kappa[L(t) - 2\pi R_0] - P_s(t). \tag{4}$$

2.1. *Expansions*

The right-hand side of the last equation requires the expansion of the curvature and the membrane length. These are given respectively by

$$\kappa = \frac{R^2 + 2(R_\theta)^2 - RR_{\theta\theta}}{[R^2 + (R_\theta)^2]^{3/2}}$$
$$L(t) = \int_0^{2\pi} (R^2 + (R_\theta)^2)^{1/2}\, d\theta.$$

We assume the membrane is a small perturbation of the unit circle, so we make the identification $R(\theta, t) = 1 + \varepsilon F(\theta, t)$. The incompressibility of the fluids imposes a constraint on F; namely, the conservation of area inside the membrane,

$$\pi = \frac{1}{2}\int_0^{2\pi} (1 + \varepsilon F)^2\, d\theta,$$

from which we deduce that

$$\int_0^{2\pi} \varepsilon F\, d\theta = -\frac{\varepsilon^2}{2}\int_0^{2\pi} F^2\, d\theta. \tag{5}$$

This equation is used in the expansion of the membrane length.

The full expansion of the equations is accomplished by writing $R = 1 + \varepsilon F^{(1)} + \varepsilon^2 F^{(2)} + \varepsilon^3 F^{(3)}$, $\phi = \varepsilon(\phi^{(1)} + \varepsilon\phi^{(2)} + \varepsilon^2\phi^{(3)})$, $\psi = \varepsilon(\psi^{(1)} + \varepsilon\psi^{(2)} + \varepsilon^2\psi^{(3)})$, and $P_s(t) = P^{(0)}(t) + \varepsilon P^{(1)}(t) + \varepsilon^2 P^{(2)}(t) + \varepsilon^3 P^{(3)}(t) + \cdots$. This leads to Poisson problems with Neumann boundary conditions for ϕ and ψ plus a matching condition that yields an equation for $F(\theta, t)$ at each order of ε. Further details of the problem definition at each order of ε are found in the Appendix.

In order to reveal the structure of the right-hand side of Eq. (4), the length of the membrane can be expanded as $L(t) - 2\pi R_0 = 2\pi\beta + \varepsilon^2 J_2 + \varepsilon^3 J_3 + \varepsilon^4 J_4 + \cdots$, where

TABLE I
Right-Hand Side of Eq. (6), Assuming $\beta_0 = O(1)$

$\beta \equiv 1 - R_0$	m	Leading orders of the right-hand side of Eq. (6)
β_0	0	$[P^{(1)} - 2\pi\beta_0 K_1] + \varepsilon[\pi\beta_0 K_2 + J_2 - P^{(1)}]$
$\beta_0\varepsilon$	$\frac{1}{2}$	$[J_2 - P^{(2)} - 2\pi\beta_0 K_1] + \varepsilon[\pi\beta_0 K_2 - K_1 J_2 + J_3 - P^{(3)}]$
$\beta_0\varepsilon^2$	1	$[J_3 - P^{(3)} - (2\pi\beta_0 + J_2)K_1] + \varepsilon[\pi\beta_0 K_2 + \frac{1}{2}K_2 J_2 - K_1 J_3 + J_4 - P^{(4)}]$
$\beta_0\varepsilon^3$	1	$[J_3 - P^{(3)} - J_2 K_1] + \varepsilon[-2\pi\beta_0 K_1 + \frac{1}{2}K_2 J_2 - K_1 J_3 + J_4 - P^{(4)}]$
$\leq\beta_0\varepsilon^4$	1	$[J_3 - P^{(3)} - J_2 K_1] + \varepsilon[\frac{1}{2}K_2 J_2 - K_1 J_3 + J_4 - P^{(4)}]$

Note. For each case, the time must be scaled by a factor of ε^m.

$$\beta = 1 - R_0 \leq 1$$

$$J_2 = \frac{1}{2}\int_0^{2\pi} [(F_\theta^{(1)})^2 - (F^{(1)})^2]\, d\theta,$$

$$J_3 = \frac{1}{2}\int_0^{2\pi} [2(F_\theta^{(1)})(F_\theta^{(2)}) - 2F^{(1)}F^{(2)} - F^{(1)}(F_\theta^{(1)})^2]\, d\theta,$$

$$J_4 = \frac{1}{8}\int_0^{2\pi} [4(F^{(1)})^2(F_\theta^{(1)})^2 + 4(F_\theta^{(2)})^2 + 8F_\theta^{(1)}F_\theta^{(3)} - 4(F^{(2)})^2 - 4(F_\theta^{(1)})^2F^{(2)} - 8F^{(1)}F^{(3)} - 8F^{(1)}F_\theta^{(1)}F_\theta^{(2)} - 4(F_\theta^{(1)})^4]\, d\theta,$$

and the curvature is $\kappa = 1 - \varepsilon K_1 + (\varepsilon^2/2)K_2 + (\varepsilon^3/2)K_3 + \cdots$, where

$$K_1 = F^{(1)} + F_{\theta\theta}^{(1)},$$

$$K_2 = (F_\theta^{(1)})^2 + 2(F^{(1)})^2 + 4F^{(1)}F_\theta^{(1)} - 2F^{(2)} - 2(F_{\theta\theta}^{(2)}),$$

$$K_3 = 4F^{(1)}F^{(2)} + 4F^{(1)}F_{\theta\theta}^{(2)} + 4F_{\theta\theta}^{(1)}F^{(2)} + 2F_\theta^{(1)}F_\theta^{(2)} - 2(F^{(1)})^3 - 3F^{(1)}(F_\theta^{(1)})^2 - 6(F^{(1)})^2F_{\theta\theta}^{(1)} + 3(F_\theta^{(1)})^2F_{\theta\theta}^{(1)} - 2F^{(3)} - 2F_{\theta\theta}^{(3)}.$$

The right-hand side of Eq. (4) is given by

$$\begin{aligned}\kappa(L(t) - 2\pi R_0) - P_s(t) = {} & [2\pi\beta - P^{(0)}] - \varepsilon[2\pi\beta K_1 - P^{(1)}] \\ & + \varepsilon^2[\pi\beta K_2 + J_2 - P^{(2)}] + \varepsilon^3[\pi\beta K_3 - K_1 J_2 + J_3 - P^{(3)}] \\ & + \frac{\varepsilon^4}{2}[4\pi\beta K_4 + K_2 J_2 - 2K_1 J_3 + 2J_4 - 2P^{(4)}] \\ & + \frac{\varepsilon^5}{2}[4\pi\beta K_5 + K_3 J_2 + K_2 J_3 - 2K_1 J_4 + 2J_5 - 2P^{(5)}] + \cdots.\end{aligned} \tag{6}$$

We infer from Eqs. (1)–(3) and Eq. (6) that the additional scaling $t' = \varepsilon^m t$, $\phi = \varepsilon^m\phi'$, and $\psi = \varepsilon^m\psi'$ for some $m \geq 1$ may be necessary whenever β is much smaller than $O(1)$ (i.e., a power of ε). The correct value of m is found from Eq. (4) and depends on the leading order of the right-hand side shown in Eq. (6). Table I shows

various cases. The pressure terms $P^{(i)}(t)$ are the ones that cancel functions of time at each order of the expansion and need not be computed explicitly. Note that the terms that come from the tension (i.e., J_2, J_3, and J_4) are functions of time only. The dependence of the forces on position is in the curvature terms.

When $\beta = O(1)$ (i.e., $m = 0$ in Table I), the base solution of the problem is a circular membrane under tension. The dominant terms on the right-hand side of the equation are the ones arising from the curvature; terms that account for variations in tension do not appear in the first two orders of the right-hand side of Eq. (6). This indicates that to $O(\varepsilon^2)$ the problem is indistinguishable from one with constant tension. The opposite extreme is the case $\beta = 0$, which corresponds to a membrane whose resting length equals the circumference of the unit circle. In this case the unperturbed solution is a circular membrane whose circumference is exactly equal to its resting length and is not under tension. For small values of β, the motion is expected to occur on a longer time scale since there is little initial energy in the membrane. The time variation of the tension is embedded in the quantities J_0, J_1, and J_2.

3. SOLUTIONS TO TWO PROBLEMS

In this section we present the solution to the approximate equations for two different orders of magnitude of β. More details are found in the Appendix. The first example illustrates the case $\beta = O(1)$ and the second illustrates the case $\beta = O(\varepsilon^2)$. In both cases the initial condition is given by a perturbation of the kth mode so that the initial shape of the membrane is given by

$$(1 - \varepsilon^2/2)^{1/2} + \varepsilon \cos(k\theta)$$

and the motion is started from rest. We recall that the approximate solution is given by

$$R(\theta, t) = 1 + \varepsilon F^{(1)}(\theta, t) + \varepsilon^2 F^{(2)}(\theta, t).$$

The solution $F^{(3)}(\theta, t)$ to the $O(\varepsilon^3)$ problem will be computed only to the extent required to provide a frequency correction to $F^{(1)}(\theta, t)$ or $F^{(2)}(\theta, t)$.

3.1. *Problem* 1

We consider a single-mode perturbation of a membrane with very small resting length, corresponding to the case $\beta = O(1)$ (we must have $\beta \leq 1$). This case is common in practical applications in physiology. The current implementation of the impulse method is for two fluids of equal density, so we set both densities equal to one ($\rho_i = \rho_o = 1$). Future work includes modifying the code to account for different densities.

The $O(\varepsilon)$ solution (see the Appendix) is given by $F^{(1)}(\theta, t) = A(t) \cos(k\theta)$, where $A(t)$ is the solution to

$$\ddot{A}(t) + \omega^2 A(t) = 0, \quad A(0) = 1, \quad \dot{A}(0) = 0,$$

so that $A(t) = \cos(\omega t)$ and ω gives the linear dispersion relation

$$\omega^2 = \pi\beta k(k^2 - 1). \tag{7}$$

The solution to the $O(\varepsilon^2)$ problem is $F^{(2)}(\theta, t) = -\frac{1}{4}A^2(t) + B(t)\cos(2k\theta)$. The first term in $F^{(2)}$ represents a correction to the unit radius in the solution $R(\theta, t)$ which results from enforcing the incompressibility condition Eq. (5). In the second term, $B(t)$ satisfies the following equation with homogeneous initial conditions

$$\ddot{B}(t) + \frac{2(4k^2 - 1)}{(k^2 - 1)}\omega^2 B(t) = -\frac{1}{2}\omega^2 + \frac{(7k^2 - 4)}{2(k^2 - 1)}\omega^2 A^2(t),$$

so that

$$B(t) = \frac{5k^2 - 2}{8(4k^2 - 1)} + \frac{(7k^2 - 4)}{8(2k^2 + 1)}\cos(2\omega t) - \frac{19k^4 - 11k^2 + 1}{4(4k^2 - 1)(2k^2 + 1)}\cos(\sigma t), \tag{8}$$

where σ is the natural frequency of $B(t)$ and is related to ω by

$$\sigma^2 = \frac{2(4k^2 - 1)}{(k^2 - 1)}\omega^2.$$

The $O(\varepsilon^3)$ solution is $F^{(3)}(\theta, t) = U(t)\cos(k\theta) + W(t)\cos(3k\theta)$, where $U(t)$ satisfies the equation

$$\ddot{U}(t) + \omega^2 U(t) = -\frac{\omega^2}{4}(k^2 - 7)A(t) + \left[\frac{(7k^4 - 55k^2 + 36)}{8(k^2 - 1)}\omega^2 - \frac{\pi}{4}k(k^2 - 1)^2\right]A^3(t) + \frac{(17k^2 - 5)}{2(k^2 - 1)}\omega^2 A(t)B(t) - \dot{A}(t)\dot{B}(t).$$

Since $A(t)$ is a solution of the homogeneous version of this equation, the presence of a term of the form $C_1 A(t)$ on the right-hand side will force the solution $U(t)$ to have a secular term. One way to remove the secularity is to use the Lindstedt–Poincaré method [15] and to introduce a new time τ at the beginning of the derivation, such that $t = \tau(1 + \varepsilon^2\omega_1)$. The effect of the new time scale is to augment the equation for $U(t)$ by the term $[-2\omega^2\omega_1 A(t)]$ on the right-hand side. The appropriate choice for ω_1 is the one that cancels the term containing $A(t)$. This value of ω_1 provides a correction to the frequency of $A(t)$ so that $A(t) = \cos((1 - \varepsilon^2\omega_1)\omega t)$. For this problem we obtain

$$\omega_1 = \frac{(k^2 - 1)(52k^4 + 65k^2 - 18)}{32(4k^2 - 1)(2k^2 + 1)} - \frac{3(k^2 - 1)}{32\beta}.$$

We recall that in this problem we assumed $\beta = O(1)$. However, since the correction was derived for $|\varepsilon^2\omega_1| \ll 1$, the result is valid for $O(\varepsilon^2) < \beta \leq 1$.

3.2. *Problem* 2

We consider a single-mode perturbation of a membrane and set $\beta = \beta_0\varepsilon^2$. This means that the difference between the circumference of the base solution and the resting length of the membrane is only $2\pi\beta_0\varepsilon^2$. The motion is, therefore, expected to be slower than in the previous problem and time must be rescaled by a factor of ε as indicated in Table I.

The $O(\varepsilon)$ solution is given by $F^{(1)}(\theta, t) = A(t)\cos(k\theta)$, where $A(t)$ is the solution to

$$\ddot{A}(t) + \omega^2 A(t) + \gamma^2 A^3(t) = 0, \quad A(0) = 1, \quad \dot{A}(0) = 0,$$

so that $A(t) = \mathrm{cn}(\eta t; p^2)$ (Jacobian elliptic cosine with modulus p; see [5]), where $\eta^2 = \omega^2 + \gamma^2$ and

$$\omega^2 = \pi\beta_0 k(k^2 - 1), \quad \gamma^2 = \frac{\pi}{4}k(k^2 - 1)^2, \quad p^2 = \frac{\gamma^2}{2\eta^2}. \tag{9}$$

The solution to the $O(\varepsilon^2)$ problem is $F^{(2)}(\theta, t) = -\frac{1}{4}A^2(t) + B(t)\cos(2k\theta)$. The first term again comes from the incompressibility condition and $B(t)$ satisfies the equation with homogeneous initial conditions

$$\ddot{B}(t) + \frac{2(4k^2 - 1)}{(k^2 - 1)}[\omega^2 + \gamma^2 A^2(t)]B(t) = -\frac{1}{4}(2\omega^2 + \gamma^2) + \frac{A^2(t)}{4(k^2 - 1)}[2\omega^2(7k^2 - 4) + \gamma^2(13k^2 - 7)A^2(t)]. \tag{10}$$

The homogeneous equation for $B(t)$ is of Lamé type (see [13, 2]) and its solutions are generally represented as infinite series in powers of $A^2(t)$.

The $O(\varepsilon^3)$ solution is again $F^{(3)}(\theta, t) = U(t)\cos(k\theta) + W(t)\cos(3k\theta)$, where $U(t)$ satisfies the equation of the form

$$\ddot{U}(t) + [\omega^2 + 3\gamma^2 A^2(t)]U(t) = H_2(A(t), B(t)).$$

We found that the secular term in the solution of this equation is of the form $[C_1 t + C_2 E(t, p)]\dot{A}(t)$, where $E(t, p)$ is the incomplete elliptic integral of the second kind, which grows roughly linearly in time. The same technique used in the previous problem can be used to remove the secularity. In this case, however, an expression for the frequency correction to $A(t)$ is not generally available. Thus ω_1 must be computed numerically.

3.3. *The Period of* $A(t)$

From the results of the previous two sections one can infer that the general equation for the amplitude $A(t)$ is

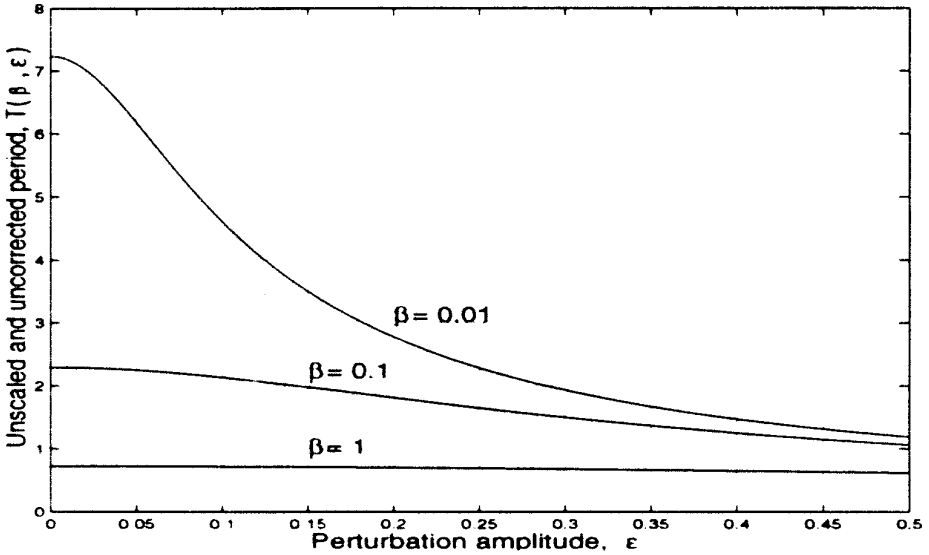

FIG. 3. $T(\beta, \varepsilon)$ vs ε for $k = 3$ and three values of β.

$$\ddot{A}(t) + \beta\omega_o^2 A(t) + \varepsilon^2\gamma^2 A^3(t) = 0, \quad A(0) = 1, \quad \dot{A}(0) = 0,$$

where

$$\omega_o^2 = \pi k(k^2 - 1), \quad \gamma^2 = \frac{\pi}{4} k(k^2 - 1)^2.$$

This equation is valid for any β such that $O(\varepsilon^2) \le \beta \le O(1)$. By retaining all three terms, one finds that the (uncorrected) period of $A(t)$ is given by

$$T(\beta, \varepsilon) = \frac{4K(p^2)}{\sqrt{\beta\omega_o^2 + \varepsilon^2\gamma^2}} \quad \text{with } p^2 = \frac{\varepsilon^2\gamma^2}{2(\beta\omega_o^2 + \varepsilon^2\gamma^2)}, \tag{11}$$

where $K(p^2)$ is the complete elliptic integral of the first kind of modulus p. In the case of $\beta = O(1)$ and $\varepsilon = 0$, this reduces to the period given by the linear dispersion relation $T = 2\pi/\omega$. In Fig. 3 the intersections of the curves with the vertical axis represent the values of the periods predicted by the linear theory. However, for a fixed $\beta \ll 1$ the finite amplitude effects are no longer negligible and a linear analysis would be appropriate only for extremely small values of the perturbation parameter ε, which would not produce appreciable motion. The nonlinear analysis in this paper was developed in order to compute the motion of the membrane for more reasonable perturbation amplitudes (e.g., $\varepsilon \approx 0.1$) and for a wide range of values of β.

4. THE IMPULSE METHOD

The numerical method we consider is the one in [9] so we present only a brief description here. Consider the incompressible Euler equations in $\mathbb{R}^2$ for a single fluid (assuming uniform unit density),

$$\mathrm{u}_t + \mathrm{u}\cdot\nabla\mathrm{u} = -\nabla p + \mathbf{F}, \quad \nabla\cdot\mathrm{u} = 0, \tag{12}$$

where u is the fluid velocity, $\nabla\cdot\mathrm{u} = 0$ is the incompressibility condition, p is the pressure, and $\mathbf{F}$ represents external force. We define $\mathbf{m}$ initially as a vector field equivalent to u up to an arbitrary gradient,

$$\mathbf{m} = \mathrm{u} + \nabla\chi, \tag{13}$$

so that u is the divergence-free part of the Hodge decomposition (see, e.g., [8]) of $\mathbf{m}$ in $\mathbb{R}^2$. The fluid velocity u is uniquely determined from $\mathbf{m}$ by finding the free-space projection of $\mathbf{m}$ onto the field of divergence-free vectors, denoted by $\mathrm{u} = \mathbb{P}\mathbf{m}$. The impulse field can be restricted to the membrane since it is there where the forces are nonzero. This impulse field is equivalent to a dipole distribution along the membrane (see [4]). The evolution equation for $\mathbf{m}$, dervied from the Euler equations and Eq. (13) (for details see [4, 9]), is

$$\mathbf{m}_t + \mathrm{u}\cdot\nabla\mathbf{m} = -(\nabla\mathrm{u})^T\mathbf{m} + \mathbf{F}, \tag{14}$$

where $\nabla\mathrm{u}$ is a matrix with entries $(\nabla\mathrm{u})_{ij} = \partial\mathrm{u}_i/\partial\mathrm{x}_j$ and T denotes the transpose.

A Lagrangian numerical method based on Eq. (14) is obtained by (a) approximating the impulse field by some discretization, (b) finding u from $\mathbf{m}$ via a projection, (c) advancing the particles and updating the impulse. The approximation of $\mathbf{m}(\mathrm{x})$ is given by a collection of impulse blobs $\tilde{\mathbf{m}}(\mathrm{x}) = \sum h^j\mathbf{m}^j f_\delta(\mathrm{x} - \mathrm{x}^j)$ centered at locations x^j. The impulse strengths $\mathbf{m}^j$ are initially set equal to the $\mathbf{m}(\mathrm{x}^j)$ and h^j represents the jth element of arclength. The cutoff function f_δ is chosen to satisfy certain conditions for the purpose of accuracy (see, e.g., [1, 3, 12, 7, 19]). In particular, an ℓth-order cutoff function is defined as $f_\delta(\mathrm{x}) = \delta^{-2}f_1(\mathrm{x}/\delta)$, where the cutoff radius δ is a small parameter and f_1 is a smooth function satisfying:

1. $\int f_1(\mathrm{x})\, d\mathrm{x} = 1$,
2. $\int \mathrm{x}^\alpha f_1(\mathrm{x})\, d\mathrm{x} = 0,\ 0 < |\alpha| < \ell - 1$,
3. $\int |\mathrm{x}|^\ell |f_1(\mathrm{x})|\, d\mathrm{x} < \infty$.

Here α is a two-dimensional multiindex and ℓ is a fixed positive integer. In this paper we use the fourth-order radially symmetric function $f_1(r) = (1/2\pi)(4e^{-r^2} - e^{-r^2/2})$.

4.1. *The Particle Velocities due to Impulse*

The projection required to find the velocity u in terms of $\mathbf{m}$ can be done exactly for a radially symmetric function f_δ. The final result is

$$\mathrm{u}(\mathrm{x}) = \sum_{j=1}^{N} h^j\mathbf{m}^j\left[\frac{rF'(r) - F(r)}{2\pi r^2}\right] - h^j\hat{\mathbf{x}}^j(\mathbf{m}^j\cdot\hat{\mathbf{x}}^j)\left[\frac{rF'(r) - 2F(r)}{2\pi r^2}\right], \tag{15}$$

where N is the total number of elements, $\hat{\mathbf{x}}^j = (\mathrm{x} - \mathrm{x}^j)/r$, $r = |\mathrm{x} - \mathrm{x}^j|$, and $F(r) =$

$\int_{|\mathbf{x}|\le r} f_\delta(|\mathbf{x}|)\, d\mathbf{x}$ is the shape factor, which depends only on the cutoff function. The particle positions are advanced using $dx^j/dt = u(x^j)$.

4.2. *The Update of Impulse Strengths*

The impulse strengths must be updated with an equation approximating Eq. (14). This is done by differentiating the expression for u to obtain the matrix ∇u, and calculating the forces at the locations x^j. The impulse strengths are updated with the equation $d\mathbf{m}^j/dt = -(\nabla u)^T\mathbf{m}^j + \mathbf{f}^j$, where $\mathbf{f}^j$ is the force on the piece of boundary represented by the jth particle (see below). For simplicity, the forces are computed at the beginning of the time step. The algorithm is:

1. For a time step Δt, compute the forces $\mathbf{f}^j$ and update the impulse strengths

$$\mathbf{m}^j \leftarrow \mathbf{m}^j + \Delta t\, \mathbf{f}^j.$$

2. Given $\tilde{\mathbf{m}}(x) = \sum_j h^j\mathbf{m}^j f_\delta(x - x^j)$, find expressions for $u(x) = \mathbb{P}\tilde{\mathbf{m}}$ and ∇u.
3. Update the particle positions and impulse strengths:

$$\frac{dx^j}{dt} = u(x^j)$$

$$\frac{d\mathbf{m}^j}{dt} = -(\nabla u)^T\mathbf{m}^j.$$

4.3. *The Computation of the Forces*

Let $\mathbf{f}$ be the force density along the elastic membrane. Then the forces exerted by the membrane on the fluid are given by the singular line integral [14]

$$\mathbf{F}(x) = \oint \mathbf{f}(s)\delta(x - x(s))\, ds, \tag{16}$$

where $x(s)$ is the arclength parametrization of the boundary and δ is the two-dimensional Dirac delta function. Given the tension $\Gamma(t)$, curvature κ, and outward unit vector normal to the boundary $\hat{n}$, the force density for Euler flow has the form $\mathbf{f}(s) = \Gamma(t)\kappa\hat{n}$. Any tangential forces make the membrane slip and do not affect the fluid motion; consequently the tension is a function of time only (see also [17]).

In practice, the forces are found at points on the boundary where impulse vectors are located. Each force vector is associated with a piece of arclength corresponding to the discretization of the boundary. The force at x^j is $\mathbf{f}^j = \Gamma(t)\kappa(x^j)h^j(t)$, where $h^j(t)$ is the discretization size of the jth particle. Each piece of arclength (the discretization size) has a stiffness constant σ and a resting length h_0 (equal for all elements). The tension is defined by the equation

$$\Gamma(t) = \sigma \sum_{j=1}^{N} (h^j(t) - h_0). \tag{17}$$

5. NUMERICAL RESULTS

Consider the case $\beta = 1$. From Section 3.1, the solution to the approximate equations is

$$r(\theta, t) = \left[1 - \frac{\varepsilon^2}{4} A^2(t)\right] + \varepsilon A(t) \cos(k\theta) + \varepsilon^2 B(t) \cos(2k\theta),$$

where for $k = 2$, $A(t)$ and $B(t)$ are

$$A(t) = \cos\left(\sqrt{6\pi}\left(1 - \frac{223}{480}\varepsilon^2\right)t\right) \tag{18}$$

$$B(t) = \frac{3}{20} + \frac{1}{3}\cos(2\sqrt{6\pi}\, t) - \frac{29}{60}\cos(\sqrt{60\pi}\, t), \tag{19}$$

and for $k = 3$ they are

$$A(t) = \cos\left(\sqrt{24\pi}\left(1 - \frac{696}{665}\varepsilon^2\right)t\right) \tag{20}$$

$$B(t) = \frac{43}{280} + \frac{59}{152}\cos(2\sqrt{24\pi}\, t) - \frac{1441}{2660}\cos(\sqrt{210\pi}\, t). \tag{21}$$

The following expressions for the membrane stretching length (L), potential energy (PE), and kinetic energy (KE) are also found to $O(\varepsilon^4)$:

$$L - 2\pi R_0 = \frac{\pi}{2}[4\beta + (k^2 - 1)\varepsilon^2 A^2(t)] \tag{22}$$

$$PE = \pi^2\beta[2\beta + (k^2 - 1)\varepsilon^2 A^2(t)] \tag{23}$$

$$KE = \pi^2\beta\varepsilon^2(k^2 - 1)[1 - A^2(t)]. \tag{24}$$

We set $\varepsilon = 0.1$. The problem was then solved with the impulse method using 600 particles with an initial spacing of $h = 0.0106$ for $k = 2$ and $h = 0.0107$ for $k = 3$. The smoothing effect of the cutoff radius on the period of the oscillations is to increase the period. This has been demonstrated numerically in [9] for the case of an interface of elliptical shape. The numerical solution was obtained for several values of the cutoff radius δ. Figures 4 and 5 show the amplitudes of the Fourier modes for $k = 2$ and $k = 3$, respectively, as compared with the asymptotic solution. The figures show that as δ decreases, the amplitudes and the frequencies approach the analytical ones. This is true for both the driving mode $A(t)$ and the driven mode $B(t)$, although the latter seems to be more sensitive to smoothing effects. We should note that the frequency of $B(t)$ has not been corrected since its correction comes at one order higher than the order of the expansion presented here. The effect of the cutoff parameter is also more pronounced for the larger perturbation frequency. This is also apparent in Fig. 6, where for $\varepsilon = 0.1$, the larger perturbation frequency

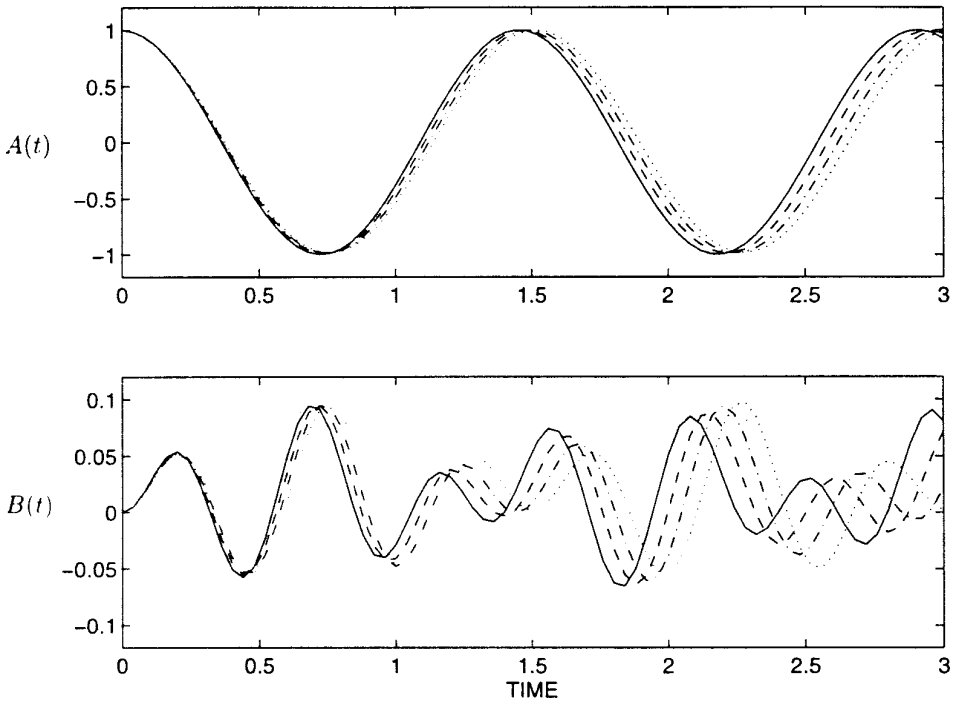

FIG. 4. Solution for $\varepsilon = 0.1$, $\beta = 1$, $k = 2$ and $\delta = 0.12$ (dotted), $\delta = 0.08$ (dash-dot), and $\delta = 0.04$ (dashed). The solid line is the expansion solution given by Eqs. (18)–(19).

($k = 3$) yields slightly larger periods relative to $k = 2$. In this figure, the periods corresponding to $\delta = 0$ have been estimated using cubic splines. From Fig. 6 we observe that for a given perturbation frequency, the results are very similar for different values of ε. This is the case because the periods in the figure have been normalized by the factor $2\pi/\omega_k$, where ω_k is the corrected frequency of $A(t)$. The area inside the membrane and the total energy in all runs were conserved to within 0.1% for $k = 2$ and within 0.2% for $k = 3$. The potential energy for both cases is shown in Fig. 7.

5.1. *Numerical Example with* $\beta = O(\varepsilon^2)$

We present examples of a k-mode perturbation of a membrane for the case $\beta = \beta_0\varepsilon^2$. This corresponds to a membrane with resting length nearly equal to the circumference of the base solution. Consequently there is little energy in the system and the motion occurs on a slow time scale. Also, the nonlinear effects of the temporal variations in the tension are present even at the leading order terms of the solution. According to Table I, time must be scaled by a factor of ε. Again we set the densities equal to 1 and solve the perturbation equations as described in Section 3.2. The solution is

$$r(\theta, t) = \left[1 - \frac{\varepsilon^2}{4}A^2(\varepsilon t)\right] + \varepsilon A(\varepsilon t)\cos(k\theta) + \varepsilon^2 B(\varepsilon t)\cos(2k\theta),$$

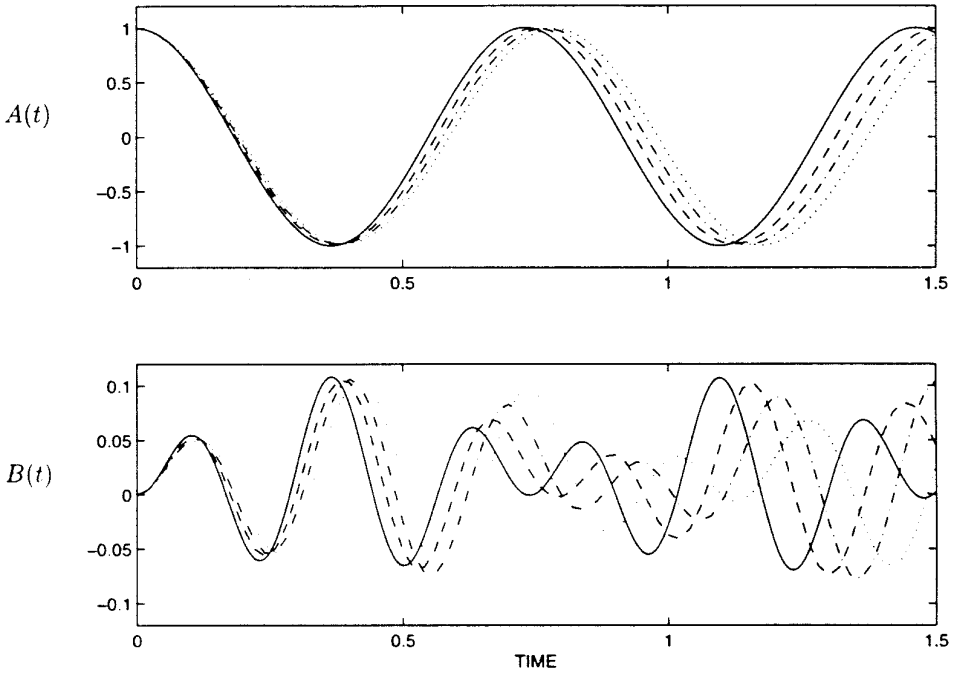

FIG. 5. Solution for $\varepsilon = 0.1$, $\beta = 1$, $k = 3$ and $\delta = 0.12$ (dotted), $\delta = 0.08$ (dash-dot), and $\delta = 0.04$ (dashed). The solid line is the expansion solution given by Eqs. (20)–(21).

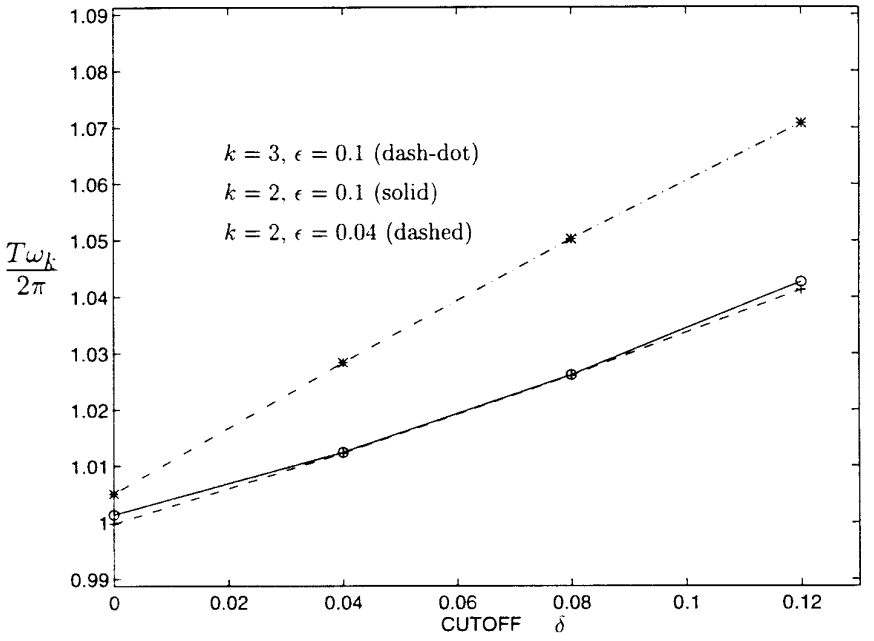

FIG. 6. Normalized period $T\omega_k/2\pi$ for two different perturbation frequencies, $\beta = 1$, $k = 2, 3$, and $\varepsilon = 0.1, 0.04$. The period T was found with the impulse method and the normalizing factors $2\pi/\omega_k$ use the corrected frequency of $A(t)$ for each case.

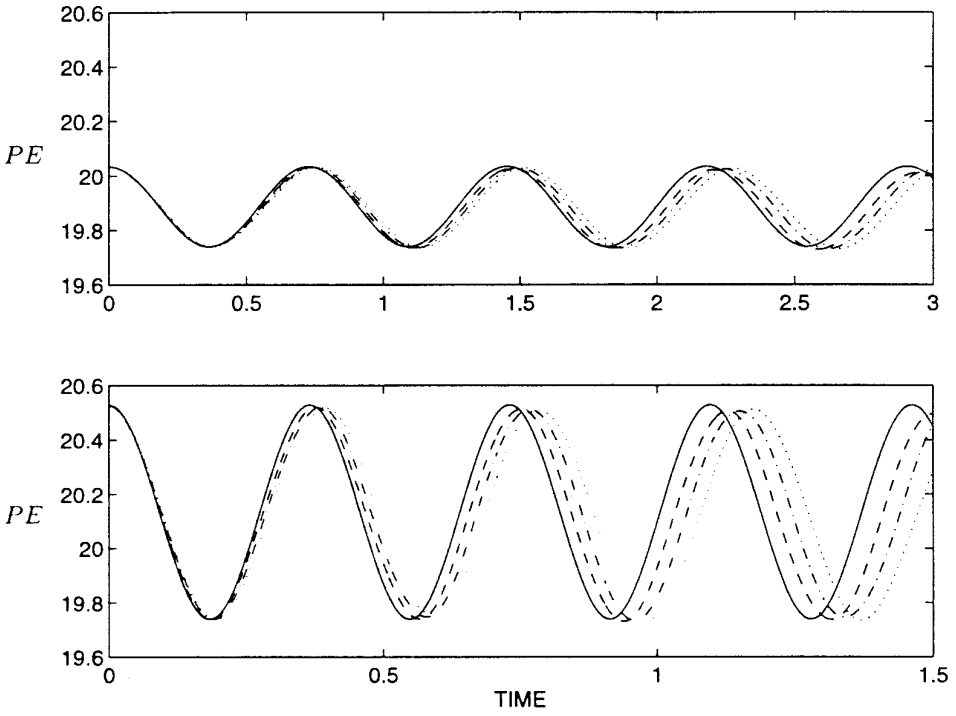

FIG. 7. Potential energy for $\beta = 1$, $k = 2$ (top), and $k = 3$ (bottom). The solid line is the expansion solution given by Eq. (23); $\delta = 0.12$ (dotted), $\delta = 0.08$ (dash-dot), and $\delta = 0.04$ (dashed); $\varepsilon = 0.1$.

where for $k = 2$, $A(t)$ is

$$A(t) = \mathrm{cn}(\sqrt{21\pi/2}(1 - 0.89668\varepsilon^2)t; 3/14) \tag{25}$$

and $B(t)$ satisfies Eq. (10) with homogeneous initial conditions. $B(t)$ was found numerically as was the correction to the frequency of $A(t)$. The value $\beta_0 = 1$ will be used throughout this section.

The approximations for the membrane length, potential energy and kinetic energy are

$$L - 2\pi R_0 = \frac{\pi\varepsilon^2}{2}[4\beta_0 + (k^2 - 1)A^2(t)] + O(\varepsilon^4) \tag{26}$$

$$PE = \frac{\pi^2\varepsilon^4}{8}[4\beta_0 + (k^2 - 1)A^2(t)]^2 + O(\varepsilon^6) \tag{27}$$

$$KE = \frac{\pi^2\varepsilon^4}{8}(k^2 - 1)(1 - A^2(t))[8\beta_0 + (k^2 - 1)(1 + A^2(t))] + O(\varepsilon^6). \tag{28}$$

This problem was solved with the impulse method using 600 particles with initial spacing $h = 0.0106$, $k = 2$, and $\varepsilon = 0.1$. A comparison of the results is shown in Fig. 8. The general characteristics of the results are similar to those of the linear problem. The numerical amplitudes and frequencies approach the ones predicted

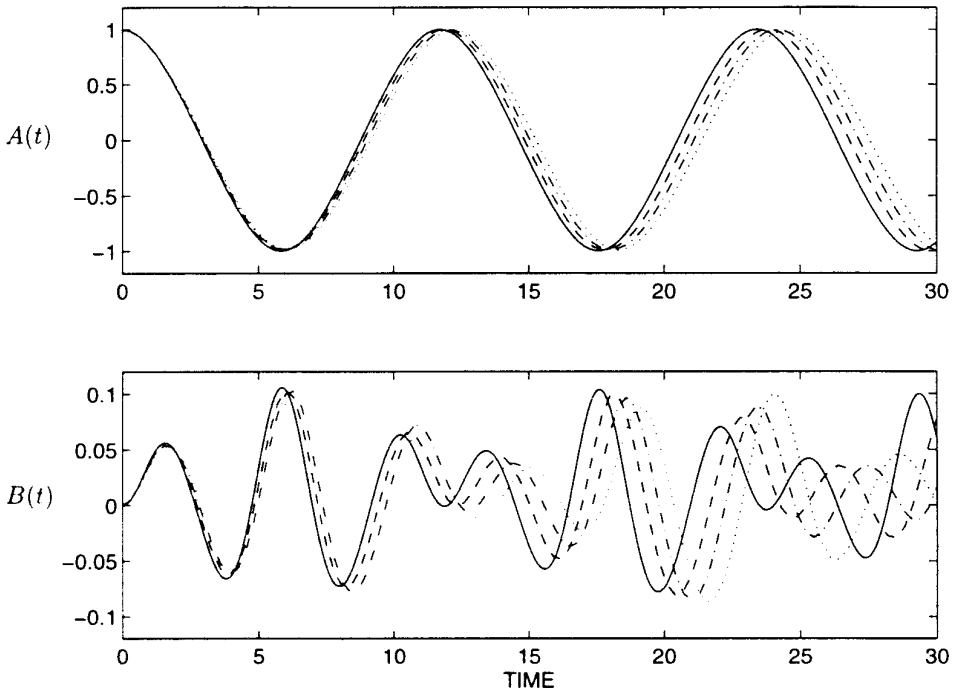

FIG. 8. Solution for $k = 2$ and $\delta = 0.12$ (dotted), $\delta = 0.08$ (dash-dot), and $\delta = 0.04$ (dashed), $\beta = \varepsilon^2$ with $\varepsilon = 0.1$. The solid line is the expansion solution given by Eq. (25) and Eq. (10).

by the perturbation analysis as δ decreases. Figure 9 shows the potential energy. In this case, the potential energy given in Eq. (27) has relative errors of size $O(\varepsilon^2)$ (multiplied by an undetermined constant) which provides only a qualitative basis for comparison. The figure shows the lag in the period and variations of the amplitudes of the numerical solution due to smoothing. The results for initial perturbation of higher modes are similar to those in the linear case. We call attention to the difference in the time scale of this problem and the previous one.

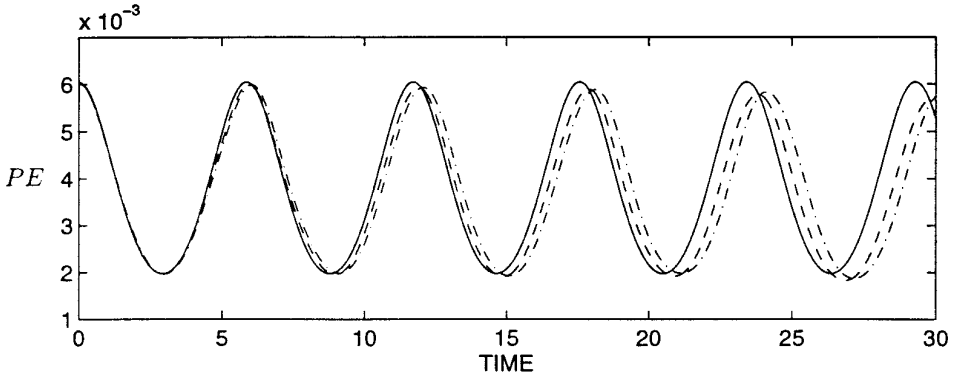

FIG. 9. Potential energy for $k = 2$ for the case $\beta = \varepsilon^2$. The solid line is the expansion solution given by Eq. (27); $\delta = 0.08$ (dash-dot) and $\delta = 0.04$ (dashed); $\varepsilon = 0.1$.

TABLE II
Numerical Periods Computed for $\varepsilon = 0.1$ Using Four Cutoff Functions of Different Orders

	Using $\delta = 0.08$	Using variable δ
Period with f_2	1.524	1.500 ($\delta = 0.0566$)
Period with f_4	1.484	1.484 ($\delta = 0.0800$)
Period with f_6	1.475	1.481 ($\delta = 0.0980$)
Period with f_8	1.471	1.480 ($\delta = 0.1131$)
Asymptotic period	1.454	1.454

Note. Here, f_k is a kth-order cutoff function as defined in Section 4. The values of δ on the third column were chosen so that all functions have the same value at the origin.

5.2. *Effect of Cutoff Functions*

In this section, we present results related to the impact of the order of the cutoff function on the solution of the problems presented earlier. The authors are not aware of any numerical studies of the choice of cutoff functions in the context of impulse methods. As discussed in Section 4, the order of a blob function f_δ is defined by the number of moment conditions it satisfies. Standard convergence proofs of vortex methods make use of this property to reduce the regularization error in the method (see, e.g., [1, 12, 19]). One family of cutoff functions has the form $f_{2n}(r) = P_{n-1}(r^2)e^{-r^2}$, where $P_n(x)$ is a polynomial of degree n. The function $\delta^{-2}f_{2n}(r/\delta)$ is a cutoff of order $2n$ [3]. The problem of Section 5 with $k = 2$, $\beta = 1$, and $\varepsilon = 0.1$ was solved again using cutoff functions of order 2, 4, 6, and 8 from this family. The impact on the period of the oscillations is displayed in Table II. The middle column shows the periods obtained with $\delta = 0.08$. One can see that significant improvement is made with the function of order 4. However, the improvement diminishes by increasing further the order of the cutoffs. Finally, the gain in using an eighth-order function over a sixth-order one is minimal. These trends are even more apparent when the cutoff parameter δ is adjusted for each function so that all of them have the same value at the origin. This normalization was suggested by Nordmark [16] in the context of vortex methods. One may argue that the high-order blobs of order up to about six reduce the regularization error significantly. The remaining discrepancy in the period is due to other sources of error in the numerical method, such as discretization errors, which increase as δ decreases (for a fixed initial particle separation).

Since the velocity field induced by an impulse vector is that of a vortex dipole with a prescribed dipole moment, the flow due to impulse can be approximated by the velocity induced by two counterrotating vortex blobs located near the base of the impulse vector [9]. Here, the vortex blobs use the same cutoff function as the impulse vector. Hence, one may expect the choice of cutoff function to play a similar role in impulse methods as it does in vortex methods. However, it is evident from Eq. (15) and Section 4 that the singularity in the impulse kernel is higher than the singularity in the vortex kernel (Biot–Savart law). Also, while the vorticity

is simply transported in two-dimensional flows, the impulse has an equation of motion which requires the computation of velocity gradients. These differences between the impulse and the vortex formulations have not had a significant effect on the size of the cutoff parameter δ (relative to the initial particle spacing) used in the computations.

6. CONCLUSIONS

We have developed a nonlinear analysis for the problem of the elastic boundary immersed in a 2D fluid. The forces along the membrane are given by the product of the curvature and a time-dependent tension, which is a function of the length of the membrane. The expansions were carried to three orders of the perturbation amplitude so that corrections to the $O(1)$ frequencies could be computed and moderately large perturbations could be studied. The dynamics of the membrane are described by the magnitude of the parameter β, which is linearly related to the resting length of the membrane. When the resting length is very small ($\beta \approx 1$), to leading order the system behaves as if the tension were constant with a response frequency given by the linear dispersion relation Eq. (7). Since the tension is a function of the stretched length of the membrane, variations of the length introduce nonlinearities to the perturbation equations. These are particularly important when the resting length of the membrane is nearly equal to the circumference of the steady solution. In this case ($\beta \ll 1$) a nonlinear dispersion relation, which includes amplitude effects, describes the dynamics of the leading mode (see Eq. (11)).

The impulse method is well-suited for this type of problem. The effect of the forces at the membrane are simply introduced as impulse density per unit of time. This numerical method as presented here requires a smoothing parameter that is typical in a Lagrangian blob method. Our results show the effect of the smoothing parameter δ on the amplitudes and the frequencies of the modes. In general, the numerical frequencies are smaller since the cutoff radius truncates large velocity gradients. This lag in the period of the motion is more pronounced for larger perturbation frequencies. The effect of the smoothing on the amplitudes is more elusive; however, the results indicate that both amplitudes and frequencies tend to the corresponding asymptotic values as the cutoff radius is decreased.

We mention, finally, two generalizations to the work presented here. One is the inclusion of viscosity into the fluid model. The viscous term in the impulse equations can be treated in a deterministic or random manner as in other particle methods. Spectral methods, for instance, are not easily adaptable to viscous flows. The second extension is to make the stiffness of the membrane a function of time. This can be included easily in the perturbation analysis. Time-dependent stiffness allows the study of problems of beating membranes and swimming motions of organisms enclosed in such membranes.

APPENDIX: THE PERTURBATION EQUATIONS

We consider a single-mode perturbation of a membrane. Let k be the mode of the perturbation so that the initial shape of the membrane is given by

$$r(\theta, 0) = (1 - \varepsilon^2/2)^{1/2} + \varepsilon \cos(k\theta)$$

and let the motion start from rest.

A.1. *The Separation of Orders*

We present details of the set of equations to be solved at each order of the expansion. The right-hand side of the dynamic condition at the interface, Eq. (6), will be denoted $\varepsilon RHS^{(1)} + \varepsilon^2 RHS^{(2)} + \varepsilon^3 RHS^{(3)}$. We recall that $\rho = \rho_o/\rho_i$.

At $O(\varepsilon)$, the equations for $x \in [0, 1)$ and $\theta \in [0, 2\pi]$ are

$$\Delta\phi^{(1)}(x, \theta, t) = 0,$$
$$\psi^{(1)}(x, \theta, t) = -\phi^{(1)}(1/x, \theta, t)$$

with conditions at $x = 1$:

$$\phi_x^{(1)} = F_t^{(1)}$$
$$(\rho + 1)\phi_t^{(1)} = -RHS^{(1)}.$$

The $O(\varepsilon^2)$ equations for $\theta \in [0, 2\pi]$ are

$$\Delta\phi^{(2)}(x, \theta, t) = \frac{1}{x}[F_{\theta\theta}^{(1)}\phi_x^{(1)} + 2F_\theta^{(1)}\phi_{x\theta}^{(1)}], \quad x \in [0, 1),$$
$$\Delta\psi^{(2)}(x, \theta, t) = \Delta\phi^{(2)}(1/x, \theta, t), \qquad x \in (1, \infty]$$

with conditions at $x = 1$:

$$\phi_x^{(2)} - \psi_x^{(2)} = 2F_\theta^{(1)}(\phi_\theta^{(1)} - \psi_\theta^{(1)})$$
$$\phi_x^{(2)} = F_t^{(2)} + F^{(1)}F_t^{(1)} + F_\theta^{(1)}\phi_\theta^{(1)}$$
$$\rho\psi_t^{(2)} - \phi_t^{(2)} - \tfrac{1}{2}(\rho - 1)[(F_t^{(1)})^2 - (\phi_\theta^{(1)})^2] = RHS^{(2)}.$$

The $O(\varepsilon^3)$ equations for $\theta \in [0, 2\pi]$ are

$$\Delta\phi^{(3)}(x, \theta, t) = \frac{1}{x}[\phi_x^{(1)}(F_{\theta\theta}^{(2)} - F^{(1)}F_{\theta\theta}^{(1)} - 2(F_\theta^{(1)})^2) + 2\phi_{x\theta}^{(1)}(F_\theta^{(2)} - F^{(1)}F_\theta^{(1)})$$
$$+ F_{\theta\theta}^{(1)}\phi_x^{(2)} + 2F_\theta^{(1)}\phi_{x\theta}^{(2)} - x(F_\theta^{(1)})^2\phi_{xx}^{(1)}], \quad x \in [0, 1),$$
$$\Delta\psi^{(3)}(x, \theta, t) = \frac{1}{x}[\psi_x^{(1)}(F_{\theta\theta}^{(2)} - F^{(1)}F_{\theta\theta}^{(1)} - 2(F_\theta^{(1)})^2) + 2\psi_{x\theta}^{(1)}(F_\theta^{(2)} - F^{(1)}F_\theta^{(1)})$$
$$+ F_{\theta\theta}^{(1)}\psi_x^{(2)} + 2F_\theta^{(1)}\psi_{x\theta}^{(2)} - x(F_\theta^{(1)})^2\psi_{xx}^{(1)}], \quad x \in (1, \infty],$$

with conditions at $x = 1$:

TABLE III
Expressions for ω and γ

$\beta = \beta_0, \beta_0\varepsilon$	$\omega^2 = \pi\beta_0 k(k^2 - 1)$	$\gamma^2 = 0$
$\beta = \beta_0\varepsilon^2$	$\omega^2 = \pi\beta_0 k(k^2 - 1)$	$\gamma^2 = \frac{\pi}{4} k(k^2 - 1)^2$
$\beta \le O(\varepsilon^3)$	$\omega^2 = 0$	$\gamma^2 = \frac{\pi}{4} k(k^2 - 1)^2$

$$\rho\psi_t^{(3)} - \phi_t^{(3)} - (\rho - 1)[F^{(1)}(\phi_\theta^{(1)})^2 + F_t^{(1)}F_t^{(2)}] + (\rho + 1)F_t^{(1)}F_\theta^{(1)}\phi_\theta^{(1)} - \phi_\theta^{(1)}(\rho\psi_\theta^{(2)} + \phi_\theta^{(2)})) = RHS^{(3)}$$

$$\phi_x^{(3)} = F_t^{(3)} + F^{(1)}F_t^{(2)} + F_t^{(1)}(F^{(2)} - (F_\theta^{(1)})^2) + \phi_\theta^{(1)}(F_\theta^{(2)} - F^{(1)}F_\theta^{(1)}) + F_\theta^{(1)}\phi_\theta^{(2)}$$

$$\psi_x^{(3)} = F_t^{(3)} + F^{(1)}F_t^{(2)} + F_t^{(1)}(F^{(2)} - (F_\theta^{(1)})^2) + \psi_\theta^{(1)}(F_\theta^{(2)} - F^{(1)}F_\theta^{(1)}) + F_\theta^{(1)}\psi_\theta^{(2)}.$$

A.2. *The Solution to the Problem*

We present the solution of the problems stated in the previous section. Only the solutions for $F^{(i)}$ are presented since they are the ultimate objective.

THE $O(\varepsilon)$ PROBLEM. The solution to the $O(\varepsilon)$ problem is

$$F^{(1)}(\theta, t) = A(t)\cos(k\theta),$$

where $A(t)$ is the solution to a problem of the form

$$\ddot{A}(t) + \omega^2 A(t) + \gamma^2 A^3(t) = 0, \quad A(0) = 1, \quad \dot{A}(0) = 0,$$

where ω and γ depend on the size of the resting length $2\pi(1 - \beta)$ as indicated in Table III.

THE $O(\varepsilon^2)$ PROBLEM. The solution to the $O(\varepsilon^2)$ problem is

$$F^{(2)}(\theta, t) = -\tfrac{1}{4}A^2(t) + B(t)\cos(2k\theta) + C(t)\cos(k\theta),$$

where $B(t)$ satisfies the following equation with homogeneous initial conditions

$$\ddot{B}(t) + \frac{2(4k^2 - 1)}{(k^2 - 1)}[\omega^2 + \gamma^2 A^2(t)]B(t) = -\frac{1}{4}(2\omega^2 + \gamma^2) + \frac{A^2(t)}{4(k^2 - 1)}[2\omega^2(7k^2 - 4) + \gamma^2(13k^2 - 7)A^2(t)]$$

and $C(t)$ satisfies an equation of the form

$$\ddot{C}(t) + \omega^2 C(t) + \gamma^2 C^3(t) = H_1(A(t)).$$

A multiple scales analysis [15] may be needed to eliminate any possible secular terms in the solution of the last equation with homogeneous initial conditions. This is accomplished by defining a new time scale τ, such that $t = \tau(1 + \omega_1\varepsilon + \omega_2\varepsilon^2)$ and deriving all equations in terms of τ. The equation for C gets augmented by a term containing ω_1, which is chosen to eliminate secular terms. This procedure introduces an $O(\varepsilon)$ correction to the frequency of $A(t)$.

THE $O(\varepsilon^3)$ PROBLEM. In general, the solution to the $O(\varepsilon^3)$ problem for a single-mode initial perturbation is of the form

$$F^{(3)}(\theta, t) = Y(t) + U(t)\cos(k\theta) + V(t)\cos(2k\theta) + W(t)\cos(3k\theta),$$

where the equation for $U(t)$ has the form

$$\ddot{U}(t) + [\omega^2 + 3\gamma^2 A^2(t)]U(t) = H_2(A(t), B(t)).$$

The multiple scales analysis would introduce an additional term into the equation for U. This term eliminates secularities in this equation with the appropriate choice of the parameter ω_2 in the definition of τ. This introduces an $O(\varepsilon^2)$ correction to the frequency of $A(t)$. Details of the multiple scales analysis can be found in [15].

REFERENCES

1. C. Anderson and C. Greengard, *SIAM J. Numer. Anal.* **22,** 413 (1985).
2. F. M. Arscott, *Periodic Differential Equations* (Pergamon, Oxford, 1964).
3. J. T. Beale and A. J. Majda, *J. Comput. Phys.* **58,** 188 (1985).
4. T. F. Buttke, Velocity methods: Lagrangian numerical methods which preserve the Hamiltonian structure of incompressible fluid flow, in *Vortex Flows and Related Numerical Methods*, edited by J. T. Beale, G-H. Cottet, and S. Huberson (Kluwer Academic, Amsterdam, 1993), p. 39. [NATO ASI Series C., vol. **395**]
5. P. F. Byrd and M. D. Friedman, *Handbook of Elliptic Integrals for Engineers and Scientists*, 2nd ed. (Springer-Verlag, New York, 1971).
6. Y. C. Chang, T. Y. Hou, B. Merriman, and S. Osher, *J. Comput. Phys.* **124,** 449 (1996).
7. A. J. Chorin, Vortex methods, in *Les Houches Summer School of Theoretical Physics* (Les Houches, France, 1993).
8. A. J. Chorin and J. E. Marsden, *A Mathematical Introduction to Fluid Mechanics* (Springer-Verlag, New York, 1979).
9. R. Cortez, *J. Comput. Phys.* **123,** 341 (1996).
10. L. J. Fauci, *J. Comput. Phys.* **86,** 294 (1990).
11. L. J. Fauci and A. McDonald, *Bull. Math. Biol.* **57,** 679 (1995).
12. O. H. Hald, Convergence of vortex methods, in *Vortex Methods and Vortex Motion*, edited by K. E. Gustafson and J. A. Sethian (SIAM, Philadelphia, 1991).
13. E. L. Ince, *Proc. Roy. Soc. Edinburgh* **60,** 47 (1939).
14. M. F. McCracken and C. S. Peskin, *J. Comput. Phys.* **35,** 183 (1980).
15. A. H. Nayfeh, *Perturbation Methods.* Wiley and Sons, New York, 1973.
16. H. O. Nordmark, Ph.D. thesis, University of California, Berkeley, 1988.

17. C. S. Peskin, Mathematical aspects of heart physiology, Lecture notes, Courant Institute of Mathematical Sciences, 1975.
18. C. S. Peskin and D. M. McQueen, *J. Comput. Phys.* **81,** 372 (1989).
19. E. G. Puckett, A review of vortex methods. In *Incompressible computational fluid mechanics*, R. Nicolaides and M. Ginzburger, editors, (Cambridge Univ. Press, Cambridge, 1993).
20. G. B. Whitham, *Linear and Nonlinear Waves* (Wiley, New York, 1974).
21. J. E. F. Williams and Y. Gou, *J. Fluid Mech.* **224,** 507 (1991).